Regular article

Computation of equilibrium oxidation and reduction potentials for reversible and dissociative electron-transfer reactions in solution

Paul Winget, Christopher J. Cramer, Donald G. Truhlar

Department of Chemistry and Supercomputing Institute, University of Minnesota,
207 Pleasant St. SE, Minneapolis, MN55455-0431, USA

Abstract. Equilibrium free-energy cycles relating oxidation and reduction potentials in solution to ionization potentials and electron affinities in the gas phase are constructed and the utilities of various levels of theory for computing particular free-energy changes within these cycles are discussed within the context of several examples. Emphasis is placed on the use of quantum-mechanical continuum solvation models to compute free energies of solvation. Key systems discussed include quinones, substituted anilines, substituted phenols, and reductive dechlorination reactions.

Keywords: Electrochemistry – Theory – Cell potential – Solvation – Self-consistent reaction field

Background and introduction

Many chemical reactions include one or more discrete steps where a single electron is transferred from one reacting partner to another. When the reacting partners are reasonably strongly coupled to one another, for example, two organometallic species sharing a common ligand, this process is referred to as an "inner-sphere" electron transfer. Conversely, an "outer-sphere" electron-transfer event is one where no ligand binds directly to both the donor and acceptor, and the electron effectively "hops" or tunnels from one species to the other.

Electron-transfer reactions play a major role in biology [1]. For instance, a photoinitiated electron-transfer event is the first step in photosynthesis. In addition, oxidative phosphorylation, the primary metabolic pathway for energy generation in higher organisms, includes electron-transfer cascades mediated by cytochromes. Electron-transfer reactions are similarly important in environmental chemistry, where many remedial strategies for cleaning up contaminated soils and other media involve oxidations or reductions of contaminants of anthropogenic origin that are initiated by either chemical or biological means [2, 3].

Because the electron is charged, its sudden translocation profoundly affects the charge distribution in a reacting system and, as such, electron-transfer reactions tend to be very sensitive to condensed-phase effects, for example, solvation [4]. Attempts to model the energetics of such reactions thus face a number of challenges. First, there are the potential difficulties that may arise in the modeling of open-shell species. Second, there is the need to accurately model the very strong interactions that a surrounding solvent will have with reactant and product ions. And, finally, if one is interested in the kinetics of electron transfer, one must adequately account for the different timescales over which various solute and solvent relaxations to equilibrium take place during and following the generally nonequilibrium electron-transfer event.

In this paper, we describe computational protocols for use in modeling electron-transfer reactions in condensed phases. In all instances the medium is represented by the influence of a surrounding dielectric continuum, and we discuss the advantages and disadvantages of such an approach for different problems. We both review prior work and present some new calculations for previously unreported systems.

Correspondence to: C. J. Cramer; D. G. Truhlar
e-mail: cramer@chem.umn.edu; truhlar@umn.edu

$$A^{+\bullet}{}_{(g)} + e^-{}_{(g)} \xleftarrow[\substack{thermal\ and\\entropic\\contributions}]{\substack{ionization\\potential\\plus}} A_{(g)} \qquad A_{(g)} + e^-{}_{(g)} \xrightarrow[\substack{thermal\ and\\entropic\\contributions}]{\substack{electron\\affinity\\plus}} A^{-\bullet}{}_{(g)}$$

$$\Delta G^{\circ}{}_{(s)}[A^+] \quad\downarrow \qquad\qquad \Delta G^{\circ} = 0 \quad\downarrow \qquad \Delta G^{\circ}{}_{(s)}[A] \quad\downarrow \qquad\qquad \Delta G^{\circ}{}_{(s)}[A] \quad\downarrow \qquad \Delta G^{\circ} = 0 \quad\downarrow \qquad\qquad \Delta G^{\circ}{}_{(s)}[A^-] \quad\downarrow$$

$$A^{+\bullet}{}_{(s)} + e^-{}_{(g)} \xleftarrow[]{\substack{absolute\\oxidation\\free\ energy}} A_{(s)} \qquad A_{(s)} + e^-{}_{(g)} \xrightarrow[]{\substack{absolute\\reduction\\free\ energy}} A^{-\bullet}{}_{(s)}$$
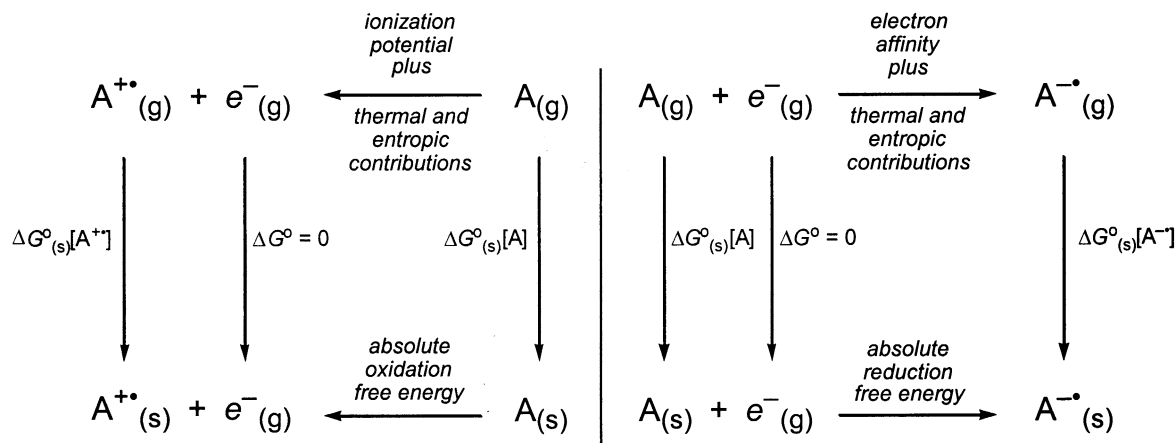
Fig. 1. Thermodynamic cycles used in the computation of equilibrium oxidation and reduction potentials

Computational protocols

We focus on the calculation of equilibrium oxidation and reduction potentials. To define a computational protocol, it is helpful to refer to one of the thermodynamic cycles, either oxidative or reductive, illustrated in Fig. 1. These cycles make clear the relationship between the condensed-phase free-energy changes associated with oxidation or reduction (the bottom legs of the illustrated cycles) and the relevant gas-phase processes.

In the gas phase, the analog to an absolute oxidation potential is an ionization potential (IP) and the analog to a reduction potential is an electron affinity (EA). By convention, however, IPs and EAs are typically reported as enthalpy changes at 0 K. In order to compute the free energy of ionization or electron attachment at 298 K (a typical temperature for the measurement of condensed-phase oxidation and reduction potentials), the 298 K thermal contributions to the free energy must be computed. With this upper leg of the free-energy cycle in hand, it is clear that the remaining connection between the gas phase and the condensed phase is simply the differential solvation free energies of the oxidized and reduced species for the process under consideration. Note that, by electrochemical convention, the free electron is always defined to be a gas-phase species for purposes of assigning absolute oxidation and reduction free energies.

Thus, in order to compute the bottom leg of the free-energy cycle, it is sufficient to compute a gas-phase free-energy change and a differential solvation free energy. Insofar as this net free-energy change in solution may be regarded as deriving from different components, it is worthwhile to note that there is not necessarily any requirement to employ identical levels of modeling in order to compute each component to an acceptable level of accuracy.

If we consider the gas-phase leg of the free-energy cycle, it seems clear that, for highest accuracy, one wants to carry out electronic structure calculations with as complete a level of theory as one can afford (i.e., attempting to converge the calculation with respect to electron correlation and a one-electron basis set). However, in order to compute the thermal contributions to free energy, it may well be possible to achieve acceptable accuracy with a considerably more efficient level of theory. The thermal contributions are most typically computed by assuming that all reacting species have partition functions characteristic of ideal gases within the rigid-rotator and harmonic-oscillator assumptions, in which case all that is required is that vibrational frequencies be determined for a molecular structure optimized at the same level of theory as that employed for the frequency calculation [5]. In favorable instances, of course, the IP may be known experimentally, in which case the computational burden for the gas-phase free-energy change reduces to computing the thermal contributions.

In order to compute equilibrium free energies of solvation for all species, self-consistent reaction field (SCRF) models based on a continuum representation of the solvent offer a particularly efficient means to achieve accuracies within a few tenths of a kilocalorie per mole for neutral species; the error is larger by approximately an order of magnitude for charged species (note that this error is about that associated with the experimental measurement of such solvation free energies) [5, 6]. Equilibrium solvation free energies are sufficient to model equilibrium oxidation and reduction free energies as these quantities are defined to refer to equilibrium conditions. In evaluating electron-transfer kinetics and in some other instances, however, it proves necessary to evaluate nonequilibrium solvation free energies [7]; such situations are outside the scope of the present article, although continuum solvation models can indeed be applied to such situations [4, 6, 8–15]. In addition, we will not discuss in any way the modeling of the dynamical events associated with electron transfer at an electrode surface, the complications associated with overpotentials for irreversible processes, the electrode double-

layer, electrolyte concentration effects, junction potentials, or other electrochemical phenomena that would be more appropriately modeled with explicit solvation models.

The absolute equilibrium oxidation or reduction free energy computed in the fashion just outlined either generates or consumes a free electron. In practice, however, free electrons are not actual participants in most reactions. Instead, the electrons are consumed, or generated, respectively, by another half-reaction. A typical half reaction is that which defines the standard hydrogen electrode (SHE)

$$H_{(aq)}^{+} + e_{(g)}^{-} \rightarrow \frac{1}{2}H_{2(g)}. \tag{1}$$

Another use of the SHE half reaction is as a reference for putting oxidation and reduction potentials on a convenient scale. On the basis of experiment, the free-energy change associated with Eq. (1) is −4.36 eV [16]. To compute a given oxidation or reduction free energy relative to the SHE, one subtracts or adds, respectively, 4.36 eV to the free-energy change computed from the thermodynamic cycles in Fig. 1 per electron transferred.

Finally, relative oxidation and reduction potentials, E^{o}, are defined as

$$E^{o} = -\frac{\Delta G^{o}}{nF}, \tag{2}$$

where ΔG^{o} is the free-energy change relative to the SHE, n is the number of electrons consumed or generated in the half-reaction of interest, and F is the Faraday constant (the negative of the charge on 1 mol of electrons). The potential is expressed in units of volts (for free energies expressed in some typical units, F is equal to 23.061 kcal mol^{-1} V^{-1} or 96.485 kJ mol^{-1} V^{-1}).

Applications to reversible redox processes

Fully computational predictions

Charles-Nicolas et al. [17] presented one of the first efforts applying the protocols just outlined; they focused on the one-electron oxidation potentials of eight polyaromatic hydrocarbons in dimethylformamide (DMF). To compute the gas-phase free-energy change, they carried out semiempirical parameterized model 3 (PM3) [18] calculations and assumed that they could neglect additional thermal terms. They further assumed that the differential free energies of solvation in DMF could be approximated by differential free energies of aqueous solvation computed using the quantum-mechanical (QM) generalized Born (GB) SCRF model PM3-SM3 [19]. Within the context of these several approximations, they achieved a mean unsigned error (MUE) in their predictions of 0.078 V. Harada et al. [20] achieved similar accuracy for a larger set of 18 polyaromatic hydrocarbons, but in

their case they added differential solvation free energies in acetonitrile computed via a QM GB model to experimental IPs.

Later, Raymond et al. [21] considered the one-electron aqueous reduction potentials of p-benzoquinone and seven of its chlorinated or methylated congeners. For all eight molecules, experimental EAs are available, and Raymond et al. found that EAs computed at the B3LYP density functional level [22–25] using the 6-311G(3d,p) basis set [26] had a MUE of 0.08 eV. As this error is below the experimental error reported for the individual EAs, Raymond et al. considered the level of electronic structure theory to be validated. They ignored thermal contributions, noting that they typically contribute less than 0.04 eV to the gas-phase reduction free energy [27]. They computed differential solvation free energies from classical simulations with explicit solvent using free-energy perturbation (FEP) [5, 28]. Over the five cases where experimental one-electron reduction potentials were available, their computed values had a MUE of 0.08 V.

Insofar as FEP calculations of differential solvation free energies are computationally expensive, we examined the degree to which QM continuum solvation models might prove useful in this system (work not previously published). Using differential solvation free energies from the QM GB SCRF model SM5.4A [29] in place of the FEP values of Raymond et al., we obtained a MUE of 0.05 V in comparison with experiment for the same five quinones. Insofar as the continuum solvation calculations require about 4 orders of magnitude less time to complete than the FEP calculations, this represents a fairly strong case for the utility of continuum solvent models in such computational schemes.

Baik and Friesner [30] recently assessed the utility of a computational protocol for eight reversible reductions of six different organic molecules in either DMF or acetonitrile solvent. The molecules together with their results are provided in Fig. 2. Note that the values in Fig. 2 do not correspond precisely to those published in their paper [30]. They reported values relative to the standard calomel electrode, which has a standard potential 0.2412 V more negative than the SHE [31], and they also employed a value of 4.43 eV for the oxidation free energy of the SHE [32, 33]; this older value has been superseded by 4.36 eV on the basis of recent, more accurate determinations of the free energy of aqueous solvation of the proton [16, 34, 35]. All values in Fig. 2 are relative to the SHE and employ an oxidation free energy of 4.36 eV for the SHE.

The computed values in Fig. 2 were arrived at by combining electronic energies computed at the B3LYP/cc-pVTZ(-f)++//B3LYP/6-31G(d,p), thermal contributions computed at the B3LYP/6-31G(d,p) level, and solvation free energies computed from solution of a SCRF Poisson equation [36, 37]. This combination gives a MUE of 0.12 V, which may be compared with the experimental error in measurement, taken in every case to be 0.04 V. Baik and Friesner noted that their errors
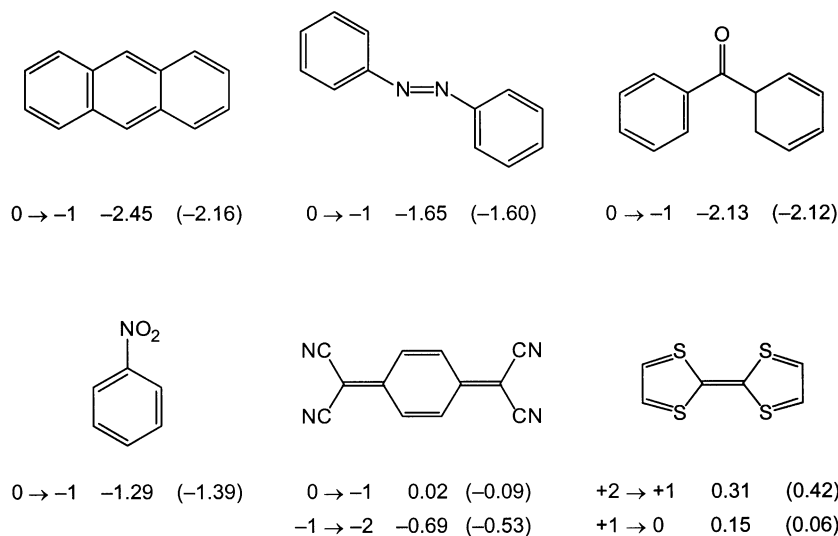
0 → −1   −2.45   (−2.16)   0 → −1   −1.65   (−1.60)   0 → −1   −2.13   (−2.12)

0 → −1   −1.29   (−1.39)   0 → −1   0.02   (−0.09)   +2 → +1   0.31   (0.42)
                         −1 → −2   −0.69 (−0.53)   +1 → 0   0.15   (0.06)

Fig. 2. Computed and experimental (in parentheses) one-electron reduction potentials relative to the standard hydrogen electrode (SHE). See the text for details of the computation

increased by 0.05 V if the diffuse functions were removed from the polarised valence-triple-ζ basis set in the single-point calculations, and by 0.2 V if the smaller 6-31G(d,p) basis set was used for the electronic energies as well as for geometries and thermal contributions.

Predictions for sets of related molecules: quinones

While the accuracy in the purely ab initio prediction of reduction potentials by Baik and Friesner is impressive, the computational cost of the protocol employed is considerable. In instances where such levels of theory may be prohibitively expensive, and where the goal is to understand variation in redox potentials over a series of chemically similar substrates, an alternative is to rely on cancellation of errors in the computation of relative redox potentials within the series. Reynolds and coworkers [38–42] provided the first comprehensive reports of such an approach, focusing on the two-electron reduction potentials of various quinones. Thus, they computed the free-energy change for the isodesmic reaction

$$Q'H_{2(aq)} + Q_{(aq)} \rightarrow Q'_{(aq)} + QH_{2(aq)} \tag{3}$$
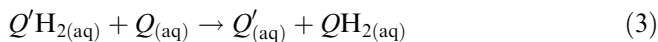
and then computed $E^{o}_{Q'}$ as

$$E^{o}_{Q'} = \frac{\Delta G^{o}}{2F} + E^{o}_{Q}, \tag{4}$$

where ΔG^{o} is the free energy change for Eq. (3) and E^{o}_{Q} is the experimental aqueous two-electron reduction potential for p-benzoquinone, 0.6998 V. In most cases, Reynolds and coworkers computed differential solvation free energies from FEP. They explored various levels of electronic structure theory for electronic energies and thermal contributions. In an initial study comparing p-benzoquinone with o-benzoquinone [38], they found Hartree–Fock (HF) and second-order perturbation theory (MP2) calculations using the 3-

(0.6998)   0.628 (0.608)

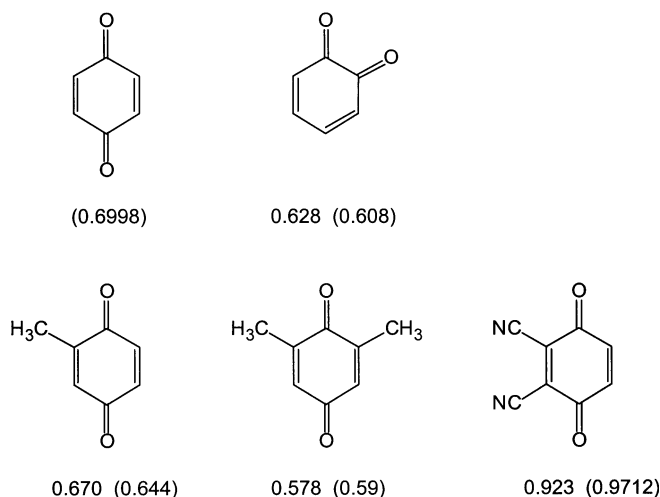0.670 (0.644)   0.578 (0.59)   0.923 (0.9712)

Fig. 3. Computed and experimental (in parentheses) aqueous two-electron reduction potentials relative to the SHE. See the text for details of the computation

21G and 6-31G(d) basis sets [5, 26] all to predict the same free-energy change for Eq. (3) to within 0.1 eV (this relatively weak dependence on basis-set size and level of theory is presumably obtained at least in part because Eq. 3 does not involve any charged species). Combining their MP2/6-31G(d) electronic energies with their FEP differential solvation free energies and thermal contributions computed at the semiempirical Austin model 1 (AM1) [43] level, they predicted a potential difference of −0.072 V, in quite good agreement with an experimental difference of −0.092 V (the statistical error in the FEP differential solvation free energies was estimated to be 0.013 V [38]). The same protocol provided similar accuracies in predicting the relative two-electron reduction potentials of 2-methyl-p-benzoquinone and 2,5-dimethyl-p-benzoquinone [39] and a somewhat larger error for 2,3-dicyano-p-benzoquinone [40], as illustrated in Fig. 3.

In a subsequent report, Reynolds [42] reconsidered these molecules and also a set of naphthoquinones. In that study, he noted that a Becke–Vosko–Wilk–Nussair density functional [22, 44] calculation gave slightly more accurate results than the MP2 method for electronic energies, and the greater efficiency of QM continnum solvation models compared with FEP was emphasized. Using PM3-SM3 [19] to compute solvation free energies Reynolds achieved a MUE of about 0.03 V over his full test set of quinones.

Jalali-Heravi and coworkers [45, 46] carried out rather similar studies to those of Reynolds and coworkers for quinones in aqueous solution, and came to overall similar conclusions. In more recent work, they went on to examine the two-electron reduction potentials of nine substituted quinones relative to 1,4-naphthoquinone in acetonitrile [47]. Using electronic energies and thermal contributions computed at the HF/6-31G(d,p) level and differential solvation free energies computed from the polarized continuum model (PCM) [48] with additional approximations for cavity, dispersion, and repulsion contributions, they obtained a MUE of 0.19 V in the predicted potentials.

Predictions for sets of related molecules: anilines

We previously reported computations of the aqueous one-electron oxidation potentials for aniline and 30 monosubstituted and disubstituted anilines employing many different levels of theory for the gas-phase and SCRF components of the calculations [49]. That work employed the older value for the absolute oxidation potential of the normal hydrogen electrode (NHE), 4.44 V [33], instead of the now preferred value of 4.36 V [16]. In addition, that prior work was subject to two errors. First, the use of an incorrect standard state for the gas-phase electron led to an error of 0.035 V in all computed potentials. In addition, the experimental data were reported as being relative to the SHE. However, the reported values were actually relative to the standard calomel electrode, which has a potential of 0.27 V relative to the SHE. Our summary of our prior results here will smaller correcting for all of these issues. This leads to smaller errors in most cases, and is the source of any discrepancies between the values noted here and those presented in the original reference [49].

Our most computationally complete protocol calculated gas-phase energies at the BPW91 [22, 50] density functional level with the cc-pVDZ basis set [51], thermal contributions at the BPW91 level with the MIDI! basis set [52], and solvation free energies with the QM GB SCRF SM5.42R/BPW91/DZVP model [53]. This protocol gave a MUE of 0.24 V for aniline and 12 monosubstituted anilines, and a MUE of 0.18 V for the three isomeric nitroanilines and six disubstituted anilines. When the much more efficient AM1 level is used for the electronic energies and the QM GB SCRF SM5.4/AM1 model is used for the aqueous solvation free energies, the MUEs increase; they are 0.49 and 0.58 V over the same two test sets noted earlier.

An interesting question, however, is the degree to which such larger errors as those associated with the semiempirical predictions may be systematic, and thus correctable given a sufficient number of data to develop some statistical correlation scheme. Indeed, it is of some interest to examine whether still simpler correlations with different experimental or computed data may be quantitatively useful in the prediction of one-electron oxidation potentials for anilines. A few likely candidates include the gas-phase IPs, the aniline pK_as, highest occupied molecular orbital (HOMO) energies from various levels of theory, and Hammett correlations [54] with the appropriate Hammett (σ) [55] and Brown (σ^+) [56, 57] parameters for substituted aromatics. The quality of linear regressions of the experimental data on these quantities, as well as on the raw computational predictions from the BPW91 and AM1 levels, is provided in Table 1 for the first test set of 13 anilines. All of the correlations provide fair to excellent agreement with experiment, as judged by comparison against the null hypothesis and the results in the previous paragraph. Least useful are the experimental gas-phase IPs (which are moreover not available for all molecules) and the AM1 HOMO energies. Linear regression on the raw predicted oxidation potentials provides the highest accuracy, and interestingly after the regression there is little difference in quality between the expensive density functional model and the very inexpensive semiempirical model. Moreover, the AM1 regression model has a slope

Table 1. Linear regressions of aqueous aniline oxidation potentials on other quantities. MUE is the mean unsigned error for the number of data indicated

Correlating variable	No. of data	Slope	Intercept	R	MUE (V)
Experimental ionization potential (eV)	9	0.23	−0.93	0.79	0.06
pK_a	13	−0.12	1.38	0.91	0.04
Hammett σ	9	0.47	0.86	0.96	0.03
Brown σ^+	8	0.32	0.90	0.98	0.02
AM1 HOMO	13	−0.24	−1.09	0.71	0.07
SM5.42R/AM1 HOMO	13	−0.81	−5.98	0.90	0.04
BPW91/MIDI! HOMO	13	−0.40	−0.95	0.85	0.05
SM5.42R/BPW91/MIDI! HOMO	13	−0.56	−1.68	0.89	0.04
AM1 + SM5.4A	13	1.03	−0.53	0.97	0.03
BPW91 + SM5.42R	13	0.62	0.50	0.99	0.02
Null hypothesis	13	[a]	0.92	[a]	0.11

[a] The null hypothesis is not a linear regression, but rather assumes every oxidation potential to be 0.92 V

near unity, suggesting that the model is accounting for substitution effects in a physical way. The slope for the density functional theory (DFT) model is substantially less than unity, which may reflect basis-set limitations and/or poor performance of the BPW91 functional.

The Hammett correlations give MUEs as low as those from these latter two computational protocols, but they are not extensible to cases of multiple substituents on the aromatic ring. When the AM1 and BPW91 regressions are applied to the computed data for the nitro-substituted and doubly substituted anilines, MUEs of 0.09 and 0.10 V, respectively, are obtained. The bulk of the excess error is associated with the nitroanilines, whose oxidation potentials are slightly more positive than any of those used to construct the regression equation.

Predictions for sets of related molecules: phenols

We now consider the utility of such simple regression schemes for the prediction of one-electron oxidation potentials in a different set of molecules, namely phenol and 23 substituted phenols. The predictions from six different theoretical protocols are compared with experiment in Table 2. In three protocols, we ignore all parts of the free-energy cycle in Fig. 1 except for the gas-phase change in electronic energy. With this approximation, we consider AM1, BPW91/MIDI!, and BPW91/cc-pVDZ. We also augment each of these levels of theory with a QM GB SCRF solvation model to compute the differential free energies of solvation of the neutral and oxidized species, in particular SM5.42R/AM1 [58], SM5.42R/BPW91/MIDI! [59], and SM5.42R/BPW91/DZVP [53].

Neglect of differential solvation effects leads to very large errors in the predicted values. This observation is unsurprising given that the cationic oxidized species is expected to have a much more favorable (negative) free energy of solvation than that of the neutral phenol. However, while inclusion of differential solvation free energies does reduce the absolute errors substantially, the MUEs nevertheless remain in excess of 0.3 V at all levels.

As differential thermal contributions rarely amount to more than several hundredths of a volt, there would seem to be some more profound error remaining in the computational protocol. Given the good performance of

Table 2. Experimental and computed aqueous one-electron oxidation potentials (volts relative to the normal hydrogen electrode) for substituted phenols. – indicates that no values were computed

	Experiment	AM1[a,b]	SM5.42R/AM1[a]	BPW 91/MIDI![a,b]	SM5.42R/BPW91/MIDI![a]	BPW91/ccpVDZ[a,b]	SM5.42R/BPW91/DZVP[a]
m-Chlorophenol	1.002	4.483	2.178	–	–	–	–
m-Ethylphenol	0.884	4.165	2.017	3.376	1.263	3.415	1.301
m-Methoxyphenol	0.887	4.074	1.999	3.012	0.992	3.115	1.096
m-Methylphenol	0.875	4.204	2.013	3.433	1.256	3.474	1.297
m-Nitrophenol	1.123	5.014	2.519	4.069	1.747	–	–
o-Chlorophenol	0.893	4.418	2.211	3.856	1.652	3.787	1.582
o-Ethylphenol	0.819	4.107	1.964	3.364	1.247	3.392	1.274
o-Hydroxybenzoate	1.113	4.394	2.240	3.490	1.419	3.642	1.570
o-Methoxyphenol	0.724	3.792	1.814	2.800	0.791	2.953	0.944
o-Methylphenol	0.834	4.109	1.948	3.392	1.220	3.431	1.259
o-Nitrophenol	1.114	5.040	2.578	–	–	–	–
o-Phenylphenol	0.831	3.806	2.037	2.910	1.101	2.960	1.151
o-*t*-Butylphenol	0.820	4.070	2.081	3.159	1.230	3.208	1.279
p-Chlorophenol	0.921	4.274	2.074	3.649	1.430	3.547	1.328
p-Ethylphenol	0.835	4.038	1.920	3.224	1.134	3.269	1.179
p-Ethylphenol	0.835	4.041	1.925	3.224	1.134	3.269	1.179
p-Hydroxyacetophenone	1.059	4.549	2.309	–	–	–	–
p-Hydroxybenzoate	0.984	4.731	2.408	–	–	–	–
p-Methoxyphenol	0.674	3.669	1.640	2.641	0.636	2.771	0.766
p-Methylphenol	0.811	4.034	1.878	3.270	1.112	3.310	1.152
p-Nitrophenol	1.192	5.173	2.740	–	–	–	–
p-Phenylphenol	0.802	3.777	1.939	2.762	0.948	2.807	0.992
p-*t*-Butylphenol	0.846	3.984	1.939	3.125	1.134	3.174	1.182
Phenol	0.901	4.291	1.994	3.648	1.338	3.700	1.390
MUE in direct predictions	0.104[c]	3.353	1.191	2.420	0.339	2.440	0.368
Linear regression data							
Slope		0.302	0.478	0.219	0.329	0.216	0.370
Intercept (V)		−0.380	−0.096	0.146	0.470	0.139	0.399
r		0.925	0.933	0.759	0.813	0.710	0.828
MUE in predictions from linear regression	0.104[c]	0.037	0.036	0.051	0.039	0.046	0.033

[a] Neglecting thermal contributions to the gas-phase portion of the free-energy cycle of Fig. 1
[b] Neglecting differential solvation free energies in the free-energy cycle of Fig. 1
[c] Error in the null hypothesis where $E^o = 0.907$ V

the DFT levels employed for calculating IPs in related molecules like the anilines just discussed [49], the only realistic factor remaining would appear to be the adequacy of the continuum approximation for computing the differential solvation free energies. We speculate that the oxidized phenols may well serve as such strong hydrogen-bond donors, insofar as they are cationic, that their specific interactions with a water molecule acting as a hydrogen-bond acceptor may be significantly stronger than those computed from the continuum model, which by its construction considers hydrogen bonding in only an average way over "typical" donor hydroxyl groups.

We have tested this suggestion with the simple model of the bimolecular complex of phenol hydrogen-bonded to a single water molecule. At the BPW91/cc-pVDZ// BPW91/MIDI! level (corresponding to column 7 of Table 2), the gas-phase oxidation potential drops from 3.70 to 3.01 V. However, differential aqueous solvation of the supermolecule radical cation versus the neutral species is smaller than for isolated phenol, so after accounting for aqueous solvation at the SM5.42R level, the oxidation potential of the supermolecule is computed as 1.23 V, a reduction of 0.16 V compared with the oxidation potential of isolated phenol. This reduction does reduce the error compared with experiment, but only by about 30%. It may be, of course, that a more sophisticated accounting of the entire first-solvent shell would recover substantial additional specific solvation effects.

To the extent that specific interactions exist, however, one might expect them to introduce a fairly systematic error into the continuum approximation. One way to correct for this error is to regress the experimental data on the computational predictions. As shown in Table 2,
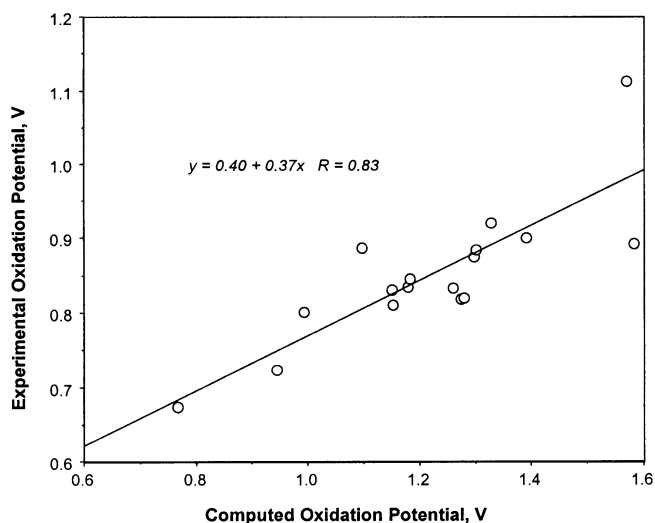
this leads in every case to regression equations with dramatically improved predictive accuracy. The MUE from all six theoretical protocols—even those which neglect to explicitly account for differential solvation effects—is less than half the MUE associated with the null hypothesis. The regression on the most complete theoretical level, BPW91/cc-pVDZ//BPW91/MIDI! with solvation effects included, provides a MUE of 0.033 V. This regression is illustrated in Fig. 4. We note that the largest outlier in the data is o-hydroxybenzoate; there may be significant issues associated with internal hydrogen bonding in this molecule.

Interestingly, the much more economical AM1 level with solvation effects included once again provides almost equivalent predictive accuracy, 0.036 V. Since six additional data are used in the AM1 regression that are not present in the DFT regression (owing to difficulties converging the open-shell Kohn–Sham determinants), this result is particularly striking. We note, however, that in every case the regression slope deviates significantly from unity, indicating that the models underestimate substitution effects in an absolute sense.

Other predictions

We close this section by noting two other studies where statistical methods were combined with relatively low level computational methods to construct predictive models having reasonable accuracy over focused data sets. Rychnovsky et al. [60] measured the reversible oxidation potentials in dichloromethane solvent of nine different nitroxyl radicals derived from piperidine. They then computed free energies of oxidation as the sum of AM1 energies of oxidation and AM1-SM2 [61] aqueous solvation free energies. When the experimental data were regressed on these computed free energies of oxidation in water, a MUE of 0.18 V in the predicted values was obtained after removal of one data point where the AM1 wave function showed high spin contamination. Rychnovsky et al. noted that in the absence of accounting for differential solvation effects with the AM1-SM2 model, there was no correlation at all between the gas-phase IPs and the measured oxidation potentials.

In a separate study, Wolfe et al. [41] trained a three-layer neural network on 58 molecules having known one-electron reduction potentials at pH 7. Input data to the neural net were the AM1 electronic energies of the neutrals and radical anions and their respective aqueous free energies of solvation as computed at the AM1-SM2 level. After having trained the net to output the one-electron reduction potential, it was used to predict E° for 23 molecules not included in the training set—primarily nitrofurans, nitrothiophenes, and nitroimidazoles. For the 11 molecules within this set for which E° had been measured, the net's mean predictive accuracy was about 0.07 V. As in our own work on the anilines and phenols, Wolfe et al. observed that lowest unoccupied molecular

Fig. 4. Computed versus aqueous one-electron oxidation potentials for substituted phenols. Computed values derive from the sum of BPW91/cc-pVDZ//BPW91/MIDI! gas-phase electronic energies and SM5.42R/BPW91/DZVP aqueous solvation free energies (thermal contributions are neglected). The best-fit line and regression equation are also shown

orbital energies were moderately anti-correlated with E^o ($r = -0.69$) and also that direct calculation from the computed free energies in aqueous solution was feasible from linear regression, the relevant equation being ($r = 0.86$)

$$E^o(\text{expt., V}) = 3.28 E^o(\text{calc., V}) + 1.068 \text{ V}. \qquad (5)$$

This correlating equation represented a substantial improvement over using simply the gas-phase EAs computed at the AM1 level ($r = 0.67$).

Applications to irreversible redox processes

Definition of equilibrium potentials

In some instances, the transfer of an electron to or from a neutral precursor leaves the resulting radical ion on an electronic ground-state surface that is dissociative. Following the electron-transfer event, which is rapid on the time scale of nuclear motion, the radical ion relaxes along the dissociative coordinate, leading to the scission of one or more bonds. Typically, the energetics associated with this fragmentation are sufficiently exergonic that the electron-transfer event is effectively irreversible. As such, techniques like cyclic voltammetry cannot be employed to define an equilibrium oxidation or reduction potential. Pulse radiolysis can occasionally be useful as a method for the fast measurement of irreversible potentials [31], but approaches along these lines are necessarily nonequilibrium in nature.

An alternative way in which to define the oxidation or reduction potential associated with a dissociative process is simply to consider the equilibrium free-energy change for the overall reaction. Thus, we may determine the free energy associated with some generic process like

$$A_{(s)} + e^-_{(g)} \rightarrow B^-_{(s)} + C^{\bullet}_{(s)} \qquad (6)$$

either by direct measurement or by knowledge of the free energies of formation of all of the reacting species. This free-energy change may then be summed with the absolute free-energy change of some particular reference electrode, for example, the NHE, and the resulting ΔG^o employed in Eq. (2) to define the relative equilibrium potential for the dissociative process.

One example of a dissociative electron-transfer reaction is the reductive dehalogenation of a chloroalkane. Such reactions are implicated in the breakdown of halocarbons in the environment, where they are typically found as residues from industrial processes. As the environmental persistence of individual halocarbons has been found to correlate with their relative reduction potentials, there has been substantial interest in the measurement and computation of these quantities [3, 62–66].

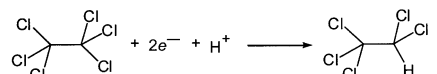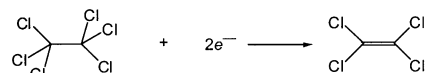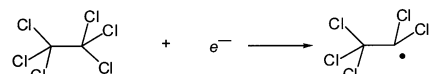From a computational standpoint, there is little difference in the protocol employed for a reversible elec-

Fig. 5. Experimental and computed aqueous one- and two-electron reduction potentials of the chlorine atom and hexachloroethane. See the text for details on the theoretical levels

tron-transfer reaction compared with that employed for an irreversible one. In either case, the free-energy cycle of Fig. 1 is applicable; it is simply that for the irreversible reaction the product of a single electron transfer is not a radical ion but rather a separated pair of one radical and one ion. For two-electron transfers, two or more closed-shell products can be generated depending on the dissociations involved.

Several examples are illustrated in Fig. 5, together with the one-electron reduction potential of the chlorine atom, as computed by Patterson et al. [66]. In these cases, electronic energies were computed at the coupled-cluster level of theory including all single and double excitations and a quasiperturbative estimate for unlinked triple excitations [67–69] using the aug-cc-pVDZ basis set [51, 70]. Geometries and thermal contributions were computed at the BPW91/aug-cc-pVDZ level, and differential solvation free energies were computed at the SM5.42R/BPW91/DZVP level. The values in Fig. 5 differ slightly from those in the original publication [66] owing to the latter using the older value of 4.44 V for the SHE; the more modern value of 4.36 V is used here. For the three reductions of hexachloroethane (HCE), the MUE in the reduction potentials is 0.06 V. The error for an aqueous chlorine atom is larger, but this derives entirely from the difficulty of computing the gas-phase EA of a monatomic species without using a very large basis set and level of electron electron.

Standard-state issues

HCE serves as a good example to illustrate some key standard-state issues that affect the numerical values associated with individual redox potentials. The first point to note is the differing concentration conventions associated with gas-phase species (like the elec-

tron, or hydrogen gas in the NHE) and species in solution. Since specification of standard-state concentration affects the numerical value of the molar translational entropy, careful attention must be paid to this issue when comparing experimental and theoretical numbers to ensure equivalent conventions in all cases. Lewis et al. [16, 71] provide a thorough discussion of this subject, and we recapitulate that here only briefly.

The typical standard-state concentration for gas-phase species is either 1 atm or 1 bar, while the typical standard-state concentration for solutes in solution is 1 M. Hence, in computing the vertical legs of the free-energy cycles in Fig. 1, it is important to ensure that the change in standard-state concentration on going from the gas phase to solution is included in the solvation free energy for solutes. Most continuum solvent models, since they focus only on the physical terms coupling the solute with the solvent, compute free energies of solvation assuming that the standard-state concentration of the solute does not change. A concentration change of 1 mol per 24.5 L (equivalent to 1 atm for an ideal gas at 298 K) to 1 mol per 1 L involves a free-energy change of $+1.9$ kcal mol^{-1}. For a reversible electron-transfer reaction like those in Fig. 1, no error is introduced if this concentration change cost is ignored in the free-energy cycle, because with only one oxidized and one reduced species the contribution cancels in the overall free-energy change in solution (recall that the free electron is defined to have a gas-phase standard state for both horizontal legs, so there is no concentration change for this species). However, for dissociative electron-transfer reactions, it is quite possible that the number of reactants may differ from the number of products, in which case such cancellation will no longer be operative.

A separate issue is that experimental measurements may sometimes be made in systems buffered to keep particular reactant or product concentrations at some value other than 1 M. Thus, for example, reductive dechlorination potentials are nearly always measured with the chloride ion concentration buffered to 10^{-3} M. To address this in a systematic way, we note that free energies computed using different concentration conventions are related by

$$\Delta G^{o\prime} = \Delta G^o + RT \ln \left(\frac{Q^{o\prime}}{Q^o} \right), \tag{7}$$

where Q is the reaction quotient (i.e., the ratio of concentrations that appear in the equilibrium constant) evaluated with all species at their standard-state concentrations and expressed so that the argument of the logarithm is dimensionless. Thus, if we consider the final reaction in Fig. 5, and take as the o standard state the 1 M convention for Cl$^-$ and take as the o$\prime$ standard state the 10^{-3} M convention, we see that the free energy in the latter case is

$$\Delta G^{o\prime} = \Delta G^o + RT \ln \left[\frac{\frac{(1\ \text{M C}_2\text{Cl}_5^\bullet)(10^{-3}\ \text{M Cl}^-)}{(1\ \text{M C}_2\text{Cl}_6)(1\ \text{M e}^-)}}{\frac{(1\ \text{M C}_2\text{Cl}_5^\bullet)(1\ \text{M Cl}^-)}{(1\ \text{M C}_2\text{Cl}_6)(1\ \text{M e}^-)}} \right]. \tag{8}$$

The final term simplifies to $RT\ln(10^{-3})$ or -4.13 kcal mol^{-1}.

Another typical experimental convention is to buffer the aqueous solution to a particular pH, for example, 7. Under those conditions, we would have for the first two-electron reduction illustrated in Fig. 5

$$\Delta G^{o\prime} = \Delta G^o + RT \ln \left[\frac{\frac{(1\ \text{M C}_2\text{Cl}_5\text{H})(10^{-3}\ \text{M Cl}^-)}{(1\ \text{M C}_2\text{Cl}_6)(10^{-7}\ \text{M H}^+)(1\ \text{M e}^-)^2}}{\frac{(1\ \text{M C}_2\text{Cl}_5\text{H})(1\ \text{M Cl}^-)}{(1\ \text{M C}_2\text{Cl}_6)(1\ \text{M H}^+)(1\ \text{M e}^-)^2}} \right], \tag{9}$$

where the final term simplifies to $RT\ln(10^4)$ or $+5.51$ kcal mol^{-1}. It is to the values computed for the o$\prime$ standard state that twice the NHE free energy of reaction is added in order to arrive at a final reduction free energy to use in Eq. (2). All of the data in Fig. 5 (experimental and theoretical) are reported for the standard state with pH 7 and a chloride concentration of 10^{-3} M.

Solvated potential-energy surfaces

One of the key strengths of computational modeling is that it can be applied not merely to the calculation of thermochemical quantities associated with equilibrium structures, but can also be used to map out interesting regions on the molecular potential-energy surface.
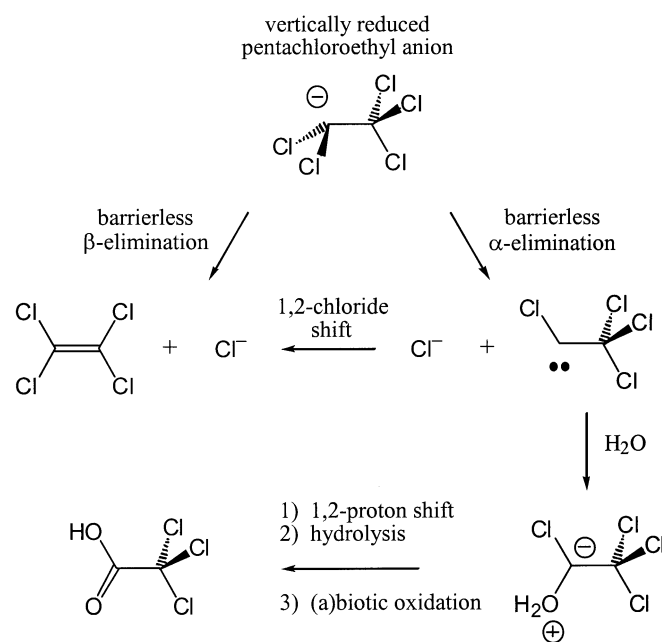

Fig. 6. Reaction channels available to the pentachloroethyl anion immediately following electron transfer

Again, HCE provides an example of a situation where theory can provide mechanistic insights not necessarily obvious from experimental analysis of the reactants and products of the reductive dechlorination reaction.

As illustrated in Fig. 6, Patterson et al. [66] determined that the vertically reduced pentachloroethyl anion—i.e., the anion having the geometry of the antecedent pentachloroethyl radical—could eject either an α or a β chloride without barrier. The latter reaction channel leads directly to a known intermediate in the reductive dechlorination of HCE, namely perchloroethylene. The former channel, however, leads to chloro(trichloromethyl)carbene. Patterson et al. determined that this carbene is a ground-state singlet having as one reaction path available to it a 1,2-chloride ion shift, this path generating perchloroethylene by a different route. The rearrangement was computed to have a modest free energy of activation in aqueous solution, about 9 kcal mol^{-1}. An alternative reaction that would be expected to be kinetically competitive is the trapping of the carbene by solvent water. The resulting ylide can rearrange and hydrolyze to trichloroacetaldehyde which, in the environment, would be expected to be very rapidly oxidized to trichloroacetic acid. On the basis of these computational results, Patterson et al. [66] proposed this mechanistic pathway to rationalize the observation of small amounts of trichloroacetic acid in product mixtures from reductive dechlorination of HCE.

Nonnenberg et al. [72] employed similar strategies to illuminate the stereoselectivity observed in the reductive dechlorination of trichloroethylene, which is observed to give as the product of two-electron reduction primarily Z-1,2-dichloroethylene and very little E or 1,1 product. Their work was carried out with density functional theory including solvation effects via the PCM model.

Concluding remarks

Continuum solvation models used in conjunction with QM calculations can provide highly accurate predictions of equilibrium one- and two-electron oxidation and reduction potentials. This accuracy can be achieved without additional approximations in cases where suitably complete levels of electronic structure theory can be employed to eliminate errors in the gas-phase predictions of IPs or EAs provided solvation of the oxidized and reduced species is well modeled by the continuum approximation. Even in instances where one or both of these conditions are not satisfied, correlations between computed and experimental data are often sufficiently high to permit useful linear or other statistical relationships between the data to be developed. Given the importance of oxidation and reduction potentials for predicting chemical reactivity, we expect steady growth in the application of computational protocols like those outlined here to the prediction of these quantities.

References

1. Zubay GL (1983) Biochemistry. Addison-Wesley, New York
2. Larson RA, Weber EJ (1994) Reaction mechanisms in environmental organic chemistry. Lewis/CRC, Boca Raton, FL
3. Page MM, Page CL (2002) J Environ Eng 128: 208
4. Marcus RA (1964) Annu Rev Phys Chem 15: 155
5. Cramer CJ (2002) Essentials of computational chemistry: theories and models. Wiley, Chichester
6. Cramer CJ, Truhlar DG (1999) Chem Rev 99: 2161
7. Marcus RA (1956) J Chem Phys 24: 979
8. Kim HJ, Hynes JT (1990) J Chem Phys 93: 5194
9. Aguilar MA, Olivares del Valle FJ, Tomasi J (1993) J Chem Phys 98: 7375
10. Rivail J-L, Rinaldi D, Dillet V (1996) Mol Phys 89: 1521
11. Klamt A (1996) J Phys Chem 100: 3349
12. Li J, Cramer CJ, Truhlar DG (2000) Int J Quantum Chem 77: 264
13. Cossi M, Barone V (2000) J Phys Chem A 104: 10614
14. Aguilar MA (2001) J Phys Chem A 105: 10393
15. Truhlar DG, Schenter, GK, Garrett, BC (1993) J Chem Phys 98: 5756 (b) Cramer CJ, Truhlar DG (1996) Understanding Chem React 17: 1 (c) Hynes, JT (1996) Understanding Chem React 17: 231 (d) Chuang Y-Y, Truhlar, DG (1999) J Am Chem Soc 121: 10157 (e) Arnold W, Winget P, Cramer CJ (2002) Environ Sci Technol 36: 3536
16. Lewis A, Bumpus JA, Truhlar DG, Cramer CJ (2004) J Chem Ed 81: 596
17. Charles-Nicolas O, Lacroix JC, Lacaze PC (1998) J Chim Phys 95: 1457
18. Stewart JJP (1989) J Comput Chem 10: 209
19. Cramer CJ, Truhlar DG (1992) J Comput Chem 13: 1089
20. Harada M, Watanabe I, Watarai H (1999) Chem Phys Lett 301: 270
21. Raymond KS, Grafton AK, Wheeler RA (1997) J Phys Chem B 101: 623
22. Becke AD (1988) Phys Rev A 38: 3098
23. Lee C, Yang W, Parr RG (1988) Phys Rev B 37: 785
24. Becke AD (1993) J Chem Phys 98: 5648
25. Stephens PJ, Devlin FJ, Chabalowski CF, Frisch MJ (1994) J Phys Chem 98: 11623
26. Hehre WJ, Radom L, Schleyer PvR, Pople JA (1986) Ab initio molecular orbital theory. Wiley, New York
27. Kebarle P, Chowdhury S (1987) Chem Rev 87: 513
28. Kollman P (1993) Chem Rev 93: 2395
29. Chambers CC, Hawkins GD, Cramer CJ, Truhlar DG (1996) J Phys Chem 100: 16385
30. Baik MH, Friesner RA (2002) J Phys Chem A 106: 7407
31. Bard AJ, Faulkner LR (2001) Electrochemical methods, fundamentals and applications. 2nd edn. Wiley, New York
32. Reiss H, Heller A (1985) J Phys Chem 89: 4207
33. Trasatti S (1986) Pure Appl Chem 58: 955
34. Tissandier MD, Cowen KA, Feng WY, Gundlach E, Cohen MH, Earhart AD, Coe JV, Tuttle TR (1998) J Phys Chem A 102: 7787
35. Tuttle TR, Malaxos S, Coe JV (2002) J Phys Chem 106: 925
36. Tannor DJ, Marten B, Murphy R, Friesner RA, Sitkoff D, Nicholls A, Ringnalda M, Goddard WA III, Honig B (1994) J Am Chem Soc 116: 11875
37. Marten B, Kim K, Cortis C, Friesner RA, Murphy RB, Ringnalda MN, Sitkoff D, Honig B (1996) J Phys Chem 100: 11775
38. Reynolds CA, King PM, Richards WG (1988) Nature 334: 80

39. Reynolds CA, King PM, Richards WG (1988) J Chem Soc Chem Commun 1434
40. Lister SG, Reynolds CA, Richards WG (1992) Int J Quantum Chem 41: 293
41. Wolfe JJ, Wright JD, Reynolds CA, Saunders ACG (1994) Anti-Cancer Drug Des 9: 85
42. Reynolds CA (1995) Int J Quantum Chem 56: 677
43. Dewar MJS, Zoebisch EG, Healy EF, Stewart JJP (1985) J Am Chem Soc 107: 3902
44. Vosko SH, Wilks L, Nussair M (1980) Can J Phys 58: 1200
45. Jalali-Heravi M, Namazian M, Peacock TE (1995) J Electroanal Chem 385: 1
46. Jalali-Heravi M, Namazian M (1997) J Electroanal Chem 425: 139
47. Namazian M, Norouzi P, Ranjbar R (2003) J Mol Struct (THEOCHEM) 625: 235
48. Miertus S, Scrocco E, Tomasi J (1981) Chem Phys 55: 117
49. Winget P, Weber EJ, Cramer CJ, Truhlar DG (2000) Phys Chem Chem Phys 2: 1231 erratum (2000) ibid 2: 1871
50. Perdew JP, Chevary JA, Vosko SH, Jackson KA, Pederson MR, Singh DJ, Fiolhais C (1992) Phys Rev B 46: 6671 erratum (1993) ibid 48: 4978
51. Dunning TH (1989) J Chem Phys 90: 1007
52. Easton RE, Giesen DJ, Welch A, Cramer CJ, Truhlar DG (1996) Theor Chim Acta 93: 281
53. Zhu T, Li J, Hawkins GD, Cramer CJ, Truhlar DG (1998) J Chem Phys 109: 9117
54. Hammett LP (1935) Chem Rev 17: 125
55. Ritchie CD, Sager WF (1964) Prog Phys Org Chem 2: 323
56. McDaniel DH, Brown HC (1958) J Org Chem 23: 420
57. Brown HC, Okamoto Y (1958) J Am Chem Soc 82: 4877
58. Hawkins GD, Cramer CJ, Truhlar DG (1998) J Phys Chem B 102: 3257
59. Li J, Zhu T, Hawkins GD, Winget P, Liotard DA, Cramer CJ, Truhlar DG (1999) Theor Chem Acc 103: 9
60. Rychnovsky SD, Vaidyanathan R, Beauchamp T, Lin R, Farmer PJ (1999) J Org Chem 64: 6745
61. Cramer CJ, Truhlar DG (1992) Science 256: 213
62. Vogel TM, Criddle CS, McCarty PL (1987) Environ Sci Technol 21: 722
63. Totten LA, Roberts AL (2001) Crit Rev Environ Sci Technol 31: 175
64. Olivas Y, Dolfing J, Smith GB (2002) Environ Toxicol Chem 21: 493
65. van Pee KH, Unversucht S (2003) Chemosphere 52: 299
66. Patterson EV, Cramer CJ, Truhlar DG (2001) J Am Chem Soc 123: 2025
67. Cizek J (1969) Adv Chem Phys 14: 35
68. Purvis GD, Bartlett RJ (1982) J Chem Phys 76: 1910
69. Raghavachari K, Trucks GW, Pople JA, Head-Gordon M (1989) Chem Phys Lett 157: 479
70. Kendall RA, Dunning TH, Harrison RJ (1992) J Chem Phys 96: 6796
71. Cramer CJ, Truhlar DG (2001) in Free Energy calculations in Rational Drug Design. Reddy MR, Erion MD (eds.) Kluwer Academic/Plenum, New York 63
72. Nonnenberg C, van der Donk WA, Zipse H (2002) J Phys Chem A 106: 8708